and ethylene. We note first that the activation energies for C-C bond scission of acetylene are the same as the activations deduced from ethane hydrogenolysis kinetics. Sinfelt's conclusion that the rate-limiting step in ethane hydrogenolysis occurred was C-C scission for a C_2H_2 species on Os and Ir, but a C_2 species on Pt is qualitatively supported by the NMR evidence for substantial hydrogen loss from acetylene on Pt prior to scission and the close agreement between activation energies for the scission of C-C bonds in adsorbed acetylene and for ethane hydrogenolysis.

Recall that there is a 6 order of magnitude difference in the rates of ethane hydrogenolysis on Pt and Ir. The NMR result that the adsorbed ethylene has the *same* energy barrier to C-C scission on Pt and Ir suggests that the species CCH_3 is not an important intermediate in ethane hydrogenolysis on Pt.

An important element in Sinfelt's analysis of ethane hydrogenolysis was the postulate that there was a quasi-equilibrium between the initial species (H_2 and C_2H_6) and the species C_2H_x undergoing C-C scission. This implies that H is going back and forth between the initial and intermediate species. Thus, one expects some population of all the intermediate species. Obviously, the populations of the various species will depend on temperature. Thus, in our annealing experiments, during the cooling step, there may be substantial population shifts. Thus, the populations we record at 77 K may differ substantially from those at higher temperatures. However, to the extent that irreversible steps occur at the annealing temperature (e.g., C-C scission), our 77 K data are reliable. For this reason, the energies of Table I are meaningful, as is the fact that some C-C scission occurs for acetylene on Pt over a broad temperature range starting at about 350 K and extending to 650 K.

Clearly, to study the reversible processes, one must do NMR measurements at reaction temperatures. Our colleague C. Klug is carrying out such studies. He has proposed that one source of C-C bond breaking on Pt below 650 K might be hydrogen-transfer reactions between adsorbed acetylene species leading to the formation of CCH_3. This species can then undergo C-C bond scission as we know from Figures 1 and 2 at temperatures above 450 K. In fact, he already has some preliminary results using ^2H NMR which show that C_2D_2 coadsorbed with H on Pt at low temperatures forms CCD_2H upon annealing. Thus, the existence of species formed by H loss from acetylene is accompanied by the possibility of formation of species containing more than two hydrogens, with the possibility of C-C bond breaking.

An intriguing possibility suggested by the above analysis is that for Ir the near coincidence of the temperatures for C-C bond scission for acetylene and ethylene may be the result of a rapid conversion of acetylene to ethylidyne followed by C-C bond scission by a process we describe above.

In conclusion, it seems clear the the NMR is observing phenomena that play a role in the kinetics of a catalytic reaction.

Acknowledgment. This research was supported by the U.S. Department of Energy, Division of Materials Research, under Contract No. DE-AC02-76ER01198, and by the Exxon Education and Research Foundation.

Registry No. C_2H_4, 74-85-1; CCH_2, 74-86-2.

High-Pressure NMR Study of Transport and Relaxation in Complex Liquids of 2-Ethylhexyl Cyclohexanecarboxylate and 2-Ethylhexyl Benzoate

J. Jonas,* S. T. Adamy, P. J. Grandinetti, Y. Masuda, S. J. Morris, D. M. Campbell, and Y. Li

Department of Chemistry, School of Chemical Sciences, University of Illinois, Champaign-Urbana, Illinois 61801 *(Received: July 11, 1989)*

The self-diffusion coefficients, densities, and shear viscosities of liquid 2-ethylhexyl cyclohexanecarboxylate (EHC) were measured as a function of pressure from 1 to 4500 bar within the temperature range from -20 to 80 °C. The Stokes-Einstein equation is applicable over 5 order of magnitude changes in self-diffusion and viscosity. The experimental data obtained are compared to those for the complex liquid of 2-ethylhexyl benzoate (EHB) in order to characterize the molecular structure effect of the replacement of the benzene ring with a saturated cyclohexyl ring. In particular, the low-temperature data suggest that conjugation of the phenyl ring with the ester group in EHB slows down diffusion and increases viscosity in comparison with EHC. Analysis in terms of the rough hard sphere model indicates a high degree of rotational-translational coupling which increases as density increases. By use of high-resolution, high-pressure NMR techniques the natural-abundance ^{13}C spin-lattice relaxation times, T_1, and nuclear Overhauser enhancement were measured for each individual carbon in EHC and EHB over the same range of temperatures and pressures. An approximate analysis of the experimental T_1 data indicates anisotropic reorientation with multiple internal rotations.

Introduction

The results of systematic NMR experiments[1,2] on studies of liquids at high pressure have provided convincing evidence about the essential role of pressure as an experimental variable in the studies of the dynamic structure of liquids. In recent papers[3,4] we presented the results of a ^1H NMR study of self-diffusion in the complex liquid of 2-ethylhexyl benzoate (EHB), the structure of which is depicted in Figure 1. Selection of EHB for this study was motivated by a lack of understanding of the relationship between the molecular properties and bulk fluid properties of elastohydrodynamic (ehd) lubricants,[5] which operate under conditions of high pressure. In this respect EHB has been chosen as a model synthetic hydrocarbon based ehd lubricant, its molecular structure being complex enough to represent a real ehd fluid while still being simple enough to allow detailed investigation of its molecular dynamics. In our study[4] we reported the self-diffusion coefficients, densities, and viscosities of liquid EHB as a function of pressure from 1 to 4500 bar within the temperature range from -20 to 100 °C. The rough hard sphere (RHS) model analysis[6] of the data indicated a high degree of coupling between the rotational and translational motions which increased as density

(1) Jonas, J. *Science* **1982**, *216*, 1179.
(2) Jonas, J. *NATO ASI, Ser. C* **1987**, *197*, 193.
(3) Walker, N. A.; Lamb, D. M.; Jonas, J.; Dare-Edwards, M. P. *J. Magn. Reson.* **1987**, *74*, 580.
(4) Walker, N. A.; Lamb, D. M.; Adamy, S. T.; Jonas, J. *J. Phys. Chem.* **1988**, *92*, 3675.
(5) Dowson, D.; Hugginson, G. R. *Elastohydrodynamic Lubrication*; Pergamon Press: London, 1977.
(6) Chandler, D. *J. Chem. Phys.* **1975**, *62*, 1358.

0022-3654/90/2094-1157$02.50/0

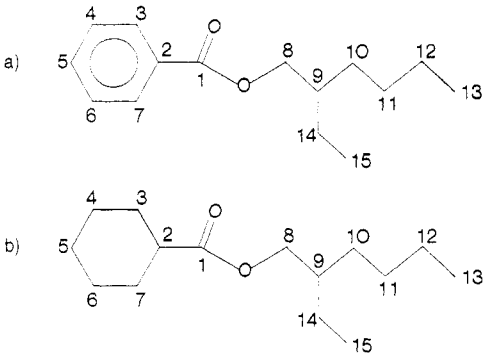

Figure 1. (a) Structural formula of EHB. (b) Structural formula of EHC. All carbons are numbered according to international organic nomenclature rules.

increased. The hydrodynamic Stokes–Einstein equation was found to be valid over 5 order of magnitude changes in self-diffusion and viscosity.

Realization of the need for improving our understanding of the relationship between molecular structure of a complex liquid and its bulk fluid properties led to the present study, which investigates the molecular dynamics in liquid 2-ethylhexyl cyclohexanecarboxylate (EHC), whose molecular structure is also given in Figure 1.

It is of interest to compare the various properties of EHC with those of EHB in order to determine the specific effect of replacing the benzene ring in EHB with a saturated, flexible cyclohexane ring in EHC. In a way analogous to our earlier study,[4] the self-diffusion coefficients, densities, and viscosities of EHC were measured by ^{1}H NMR as a function of pressure from 1 to 4500 bar within the temperature range from −20 to 80 °C. Again, the RHS model and the Stokes–Einstein equation are used to analyze the self-diffusion and viscosity data.

It is important to emphasize that 5 order of magnitude changes in self-diffusion and fluidity are covered in our experiments on EHC. This wide change in the fluidity provides a unique opportunity to investigate the relationship between the molecular level quantites, e.g., reorientational correlation times and the fluidity of the medium. The modified Debye equation[7] gives the functional dependence of the reorientational correlation times, τ_θ, upon viscosity

$$\tau_\theta = \kappa V_H(\eta/kT) + \tau_H \qquad (1)$$

where τ_θ is the rotational correlation time, V_H is the hydrodynamic volume, τ_H is the zero viscosity correlation time, and η is the shear viscosity. The McClung and Kivelson[7] parameter κ represents the ratio of the mean square intermolecular torques on the solute molecules to the mean square intermolecular forces on the solvent molecules. The total intermolecular potential energy determines both the torques and the forces, but only the anisotropic part of this potential gives rise to the torques. Therefore, the McClung and Kivelson parameter[7] reflects the extent of the coupling between the rotational and the translational motions, and in addition it provides information about the degree of anisotropy that characterizes these motions. The validity of the Debye equation has recently been investigated in our laboratory[8] in a series of complex, highly viscous liquids over a wide range of fluidity changes.

We have shown[8] that, for anisotropically reorienting molecules, the rotational–translational coupling parameter increases with increasing density, in contrast to the case of symmetric molecules which possess an axis of symmetry for relatively unhindered reorientations, for which the coupling parameter decreases with increasing density. By examining a sufficiently broad viscosity range, it has been possible to show that the rotational–translational coupling parameter is not a pressure-independent quantity, as previously reported. Under isochoric conditions, the coupling parameter was found to be insensitive to kinetic energy changes. It was concluded that volume rather than kinetic energy plays the decisive role in determining the nature and the degree of the coupling.

Both experimental[9-12] and theoretical[13-16] studies have demonstrated the value of natural-abundance ^{13}C NMR relaxation experiments to yield a wealth of information about the motional dynamics of complex liquids. So far, however, all such ^{13}C NMR studies have been performed only as a function of temperature at atmospheric pressure. Taking advantage of our recent development[17] of NMR instrumentation which permits high-resolution, high-sensitivity NMR experiments on liquids at high pressure, we decided to measure natural-abundance ^{13}C NMR spin–lattice relaxation times, T_1, and nuclear Overhauser enhancement (NOE) in liquid EHC and EHB as a function of pressure from 1 to 4500 bar within the temperature range from −20 to 80 °C. The general expressions relating ^{13}C T_1 and NOE to the spectral density functions for the intramolecular dipolar coupling mechanism are

$$\frac{1}{NT_1} = \frac{1}{10}\frac{\hbar^2\gamma_C^2\gamma_H^2}{r_{CH}^6}[J(\omega_H - \omega_C) + 3J(\omega_C) + 6J(\omega_H + \omega_C)] \qquad (2)$$

$$\mathrm{NOE} = 1 + \frac{\gamma_H}{\gamma_C}\left[\frac{6J(\omega_H + \omega_C) - J(\omega_H - \omega_C)}{J(\omega_H + \omega_C) + 3J(\omega_C) + 6J(\omega_H + \omega_C)}\right] \qquad (3)$$

where N is the number of directly attracted protons, $J(\omega)$ is the spectral density function, and ω_H and ω_C are the proton and carbon resonant frequencies, respectively. The particular form of $J(\omega)$ depends on the model for molecular reorientation. Because of asymmetric shape and high degree of internal mobility in EHC and EHB, the form of $J(\omega)$ needed to describe the relaxation is complicated.

In summary, there are several goals of the present study: first, to measure the pressure and temperature dependence of the self-diffusion coefficients, densities, and shear viscosities in liquid EHC; second, to test the validity of the Stokes–Einstein equation for EHC; third, to determine the pressure and temperature dependence of the natural-abundance ^{13}C NMR relaxation times, T_1, and NOE for each individual carbon resonance in liquid EHC and EHB; fourth, to analyze the relaxation data in terms of available theoretical models for motional dynamics in liquids; fifth, to relate the various molecular reorientational correlation times to the fluidity via the modified Debye equation; sixth, for all properties investigated, to compare the data for EHC with those for EHB in order to determine what effect the replacement of benzene with the cyclohexane ring has on the details of motional dynamics in the complex liquids studied.

Experimental Section

Materials. The EHC sample was synthesized in our laboratory, and the EHB sample was synthesized by Palmer Research Ltd. (U.K.). EHC was prepared by coupling 2-ethylhexanol with cyclohexanecarbonyl chloride in the presence of dimethylaniline. The alcohol (19.5 g, 0.15 mol) and 25 g of dimethylaniline were dissolved in 10 mL of anhydrous ethyl ether and placed in a three-neck flask. A solution of the chloride (23.1 g, 0.188 mol) in 20 mL of ethyl ether was added dropwise. The reaction mixture was kept at 35 °C overnight and washed with 10% H_2SO_4, saturated $NaHCO_3$, and water repeatedly. This was then purified

(7) McClung, R. E.; Kivelson, D. *J. Chem. Phys.* **1968**, *49*, 3380.
(8) Artaki, I.; Jonas, J. *J. Chem. Phys.* **1985**, *82*, 3360.
(9) Burnett, L. J.; Roeder, S. B. W. *J. Chem. Phys.* **1974**, *60*, 2420.
(10) Lyerla, Jr., J. R.; Horikawa, T. T. *J. Phys. Chem.* **1976**, *80*, 1106.
(11) Lyerla, Jr., J. R.; McIntyre, H. M.; Torchia, D. A. *Macromolecules* **1974**, *7*, 11.
(12) Schaefer, J. *Macromolecules* **1973**, *6*, 882.
(13) Levine, Y. K.; Partington, P.; Roberts, G. C. K. *Mol. Phys.* **1973**, *25*, 497.
(14) Levine, Y. K.; Birdsall, M.; Lee, A. G.; Metcalfe, J. C.; Partington, P.; Roberts, G. C. K. *J. Chem. Phys.* **1974**, *60*, 2890.
(15) London, R. E.; Avitable, J. *J. Chem. Phys.* **1976**, *65*, 2443.
(16) London, R. E.; Avitable, J. *J. Am. Chem. Soc.* **1977**, *99*, 7765.
(17) Jonas, J.; Xie, C.-L.; Jonas, A.; Grandinetti, P. J.; Campbell, D.; Driscoll, D. *Proc. Natl. Acad. Sci. U.S.A.* **1988**, *85*, 4115.

TABLE I: Experimental Self-Diffusion Coefficients, Viscosities, and Densities of EHC

T, °C	P, bar	η, cP	ρ, g cm^{-3}	10^9D, cm^2 s^{-1}
−20	1	27.1	0.9318	318
	500	69.4	0.9431	154
	1000	172	0.9522	861
	1500	416	0.9598	
	2000	978	0.9665	
	2500	2360	0.9724	3.00
	3000	5450	0.9776	1.03
	3500	11700	0.9824	.505
	4000	24900	0.9868	.230
	4500	53200	0.9908	.0959
40	1	4.03	0.9046	3120
	500	7.08	0.92060	1790
	1000	11.4	0.9446	1310
	1500	20.0	0.9569	583
	2000	32.9	0.9624	375
	2500	52.1	0.9777	229
	3000	78.1	0.9862	128
	3500	128	0.9943	
	4000	206	1.0027	
	4500	316	1.0088	
80	1	1.48	0.8795	7180
	500	2.23	0.9095	4350
	1000	3.59	0.9271	2720
	1500	5.86	0.9425	1960
	2000	7.36	0.9574	1320
	2500	10.5	0.9663	904
	3000	17.6	0.9747	649
	3500	27.0	0.9848	481
	4000	37.3	0.9948	330
	4500	46.1	1.0034	217

TABLE II: Parameters of the Tait Equation

T, °C	B, bar	C
−20	1460	0.1411
40	1102	0.1460
80	843.4	0.1519

by passing through a silica column and eluting with petroleum ether. The solvent was then removed at reduced pressure.

Anal. Calcd for $C_{15}H_{28}O_2$: C, 75.00; H, 11.67. Found C, 75.04; H, 11.63. High-resolution electron impact mass spectrum for calculated $C_{15}H_{28}O_2$.

Diffusion Measurements. The diffusion measurement technique is the same as discussed previously.[4] Diffusion coefficients greater than 3×10^{-8} cm^2/s were measured by the spin-echo Bessel analysis technique.[18] Diffusion coefficients less than 3×10^{-8} cm^2/s were determined by the Burnett and Harmon[19] method of measuring the H_1 field dependence of the rotating-frame proton spin-lattice relaxation time ($T_{1\rho}$). The spin-echo-derived data are estimated to be accurate to ±3% for the largest D values and to ±10% for the lowest D values. The accuracy of the $T_{1\rho}$ derived data is estimated at ± 30%. The measurements were made with ^{1}H NMR at 60 MHz in a wide-gap Varian electromagnet. Further experimental details are given in our previous paper.[4] Diffusion coefficients are listed in Table I.

Densities. A high-pressure, variable-temperature densitometer[20] was used to make the density measurements. The densitometer was calibrated by using 1-bar densities obtained with a commercially available Mettler/Paar DMA 45 digital density meter. The isothermal plots of experimental densities against pressure were fit to the Tait equation

$$(1/\rho_r - 1/\rho_p)\rho_r = C \log [(B + P)/(B + P_r)] \qquad (4)$$

where ρ_p is the density in g/cm^3 at a pressure P, ρ_r is the density at the reference pressure (P_r = 1 bar), and B and C are the Tait parameters. The fitted densities for each isotherm are shown in Table I, while the Tait parameters are shown in Table II. The accuracy of the density measurements is estimated at ±5%.

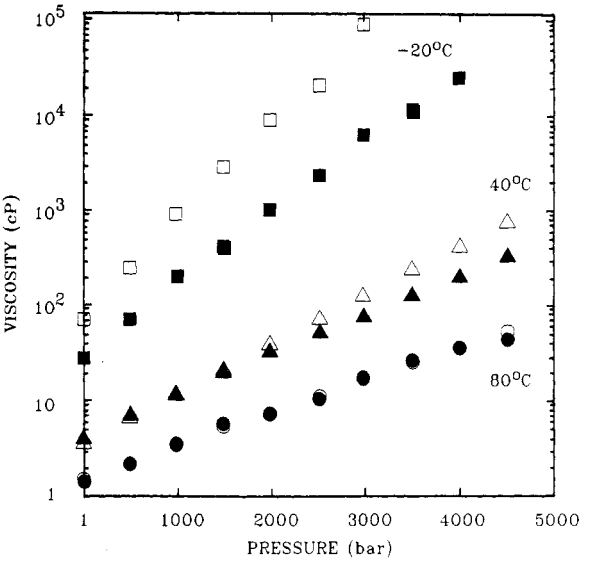

Figure 2. Pressure dependence of shear viscosity of EHC and EHB: □, EHB, −20 °C; △, EHB, 40 °C; ○, EHB, 80 °C; ■, EHC, −20 °C; ▲, EHC, 40 °C; ●, EHC, 80 °C.

Viscosities. Viscosity measurements were obtained by using a high-pressure falling-slug viscometer described previously.[8] The viscometer was calibrated throughout the range of 1–10^5 cP by using methanol, ethanol, 1-propanol, glycerol, and various silicon oils of known viscosity. All calibration runs were done at 1 bar. The accuracy of the viscosity measurements is estimated at ±10%. Viscosities are listed in Table I.

Carbon-13 NMR Measurements. Proton-decoupled carbon-13 spectra were obtained at 45.286 MHz with a home-built spectrometer interfaced to a General Electric 293D programmable pulser and a Nicolet 1280 computer. Details of the spectrometer are given elsewhere.[21] The samples were held in a high-pressure double resonance probe which is a modification of a probe discussed earlier[22,23] and described in detail by Grandinetti.[21] Spectra were obtained with a 6000-Hz spectral width and 4096 or 8192 data points for EHB and a 3000-Hz spectral width and 8192 or 16 384 data points for EHC. Carbon-13 spin–lattice relaxation times were measured with the use of a $\pi-\tau-\pi/2$ pulse sequence, with the π-pulse being a composite pulse which compensated for any inhomogeneity in the H_1 field. Finally, nuclear Overhauser enhancements were obtained by using a gated decoupler routine. The T_1 and NOE values are accurate to within 10%.

As in the proton NMR diffusion measurements, pressures up to 5000 bar were generated with hand-operated pumps and a pressure intensifier. The degassed sample was separated from the pressure transmitting fluid, carbon disulfide, by use of stainless steel bellows sealed to a glass sample cell.[24] Pressures are accurate to ±10 bar and were measured with a Heise-Bourdon gauge. Temperatures were maintained by circulating either an ethylene glycol–water mixture (for higher temperatures) or methanol (for lower temperatures) through a jacket surrounding the bomb. The temperatures, accurate to ±0.5 °C, were measured with a thermocouple located slightly above the sample within the high-pressure environment. Before any measurements were made, the sample was allowed to equilibrate for at least 1 h.

Results and Discussion

Transport Properties. Table I gives the diffusion coefficients, shear viscosities and densities of EHC in the pressure range 1–4500 bar and the temperature range from −20 to 80 °C. It is important to emphasize that similarly, as in the case of the EHB liquid, the

(18) Lamb, D. M.; Grandinetti, P. J.; Jonas, J. *J. Magn. Reson.* **1987**, *72*, 532.
(19) Burnett, L. J.; Harmon, J. F. *J. Chem. Phys.* **1972**, *57*, 1293.
(20) Parkhurst, H. J.; Jonas, J. *J. Chem. Phys.* **1975**, *63*, 2698.
(21) Grandinetti, P. J. Ph.D. Thesis, University of Illinois, 1988.
(22) Jonas, J.; Hasha, D. L.; Lamb, W. J.; Hoffman, G. A.; Eguchi, T. *J. Magn. Reson.* **1981**, *42*, 169.
(23) Vander Velde, D. G.; Jonas, J. *J. Magn. Reson.* **1987**, *71*, 480.
(24) Jonas, J. *Rev. Sci. Instrum.* **1972**, *43*, 643.

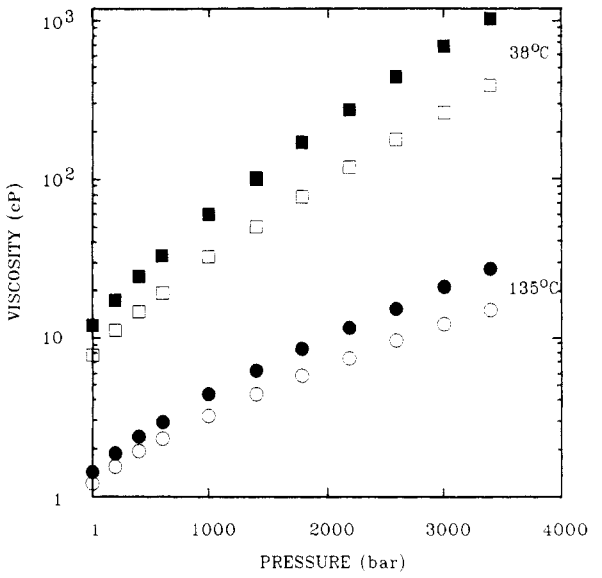

Figure 3. Pressure dependence of viscosity of (2-cyclohexylethyl)heptadecane (CEH) and (2-phenylethyl)heptadecane (PEH): ■, CEH, 38 °C; ●, CEH, 135 °C; □, PEH, 38 °C; ○, PEH, 135 °C.

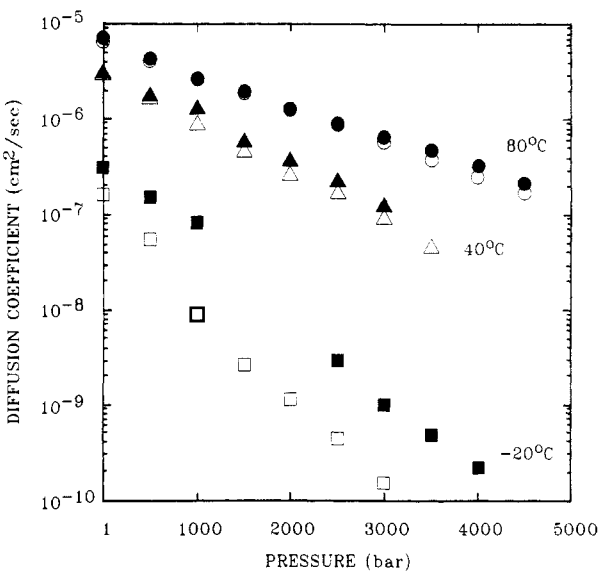

Figure 4. Pressure dependence of self-diffusion in EHC and EHB: □, EHB, −20 °C, △, EHB, 40 °C; ○, EHB, 80 °C; ■, EHC, −20 °C; ▲, EHC, 40 °C; ●, EHC, 80 °C.

TABLE III: Comparison of Compressibilities for EHB, EHC, PEH,[a] and CEH[a]

P, bar	k,[b] × 10^5 bar^{-1}			
	EHB	EHC	PEH	CEH
1	5.72 (−20)	4.19 (−20)	6.79 (38)	7.00 (38)
3000	2.24 (−20)	1.47 (−20)	2.27 (38)	2.30 (38)
1	9.73 (80)	7.81 (80)	11.8 (135)	12.1 (135)
3000	2.82 (80)	1.90 (80)	2.71 (135)	2.73 (135)

[a] k values taken from ref 26. [b] Temperatures in °C are given in parentheses after the k value.

range of viscosities and diffusion coefficients measured is approximately 5 orders of magnitude. Since one of the main goals of the study is to determine the effects of replacing the benzene ring in the EHB liquid with a cyclohexane ring in the EHC liquid, we present Figure 2, which compares the shear viscosities of EHC and EHB over the studied range of pressures and temperatures. Inspection of this figure shows that the shear viscosities for EHB and EHC are nearly identical at 80 °C, but one finds significant difference in η at the low temperature −20 °C where EHB has higher viscosities, and the difference increases with the increasing pressure. Even at 40 °C one detects a difference in η between EHB and EHC at higher pressures. It is interesting to compare this behavior with that reported for a (2-phenylethyl)heptadecane (PEH) and a (2-cyclohexylethyl)heptadecane (CEH) as reported by Lowitz et al.[25] From Figure 3, one can see that the opposite is true for viscosities of PEH and CEH, the viscosity of the hydrocarbon fluid CEH with the cyclohexane ring being higher than that of the phenyl containing PEH liquid.

Another property that is distinctly different for EHC and EHB is compressibility. For illustration, we include Table III, which compares compressibilities, k, of EHB and EHC with those[26] of PEH and CEH at selected pressures and temperatures. Clearly, compressibilities of EHB liquid are higher than those of EHC. This again contrasts to the k, values reported[26] for PEH and CEH where the difference in k is very small, and k for CEH appears to be slightly higher than that of PEH.

The different behavior of EHB and EHC when compared to the behavior of PEH and CEH fluids must be due to the fact that in EHB there is a possibility of conjugation of the phenyl with the ester group which results in a hindered rotation about the C–C bond between the phenyl and the carbonyl group. Several resonant structures exist for EHB and particularly at lower temperatures the rotation about the C–C bond will be slow, so that the C_6H_5COO part of the molecule represents a relatively rigid planar structure. Since no such conjugation can occur in EHC, PEH, and CEH, this explains the observed differences in viscosity and compressibility behavior. This interpretation is also supported by the experimental T_1 data discussed later in this study.

The self-diffusion coefficients of EHC and EHB measured as a function of pressure and temperature exhibits a behavior consistent with that observed for shear viscosity as discussed above. As it is shown in Figure 4, EHC diffuses faster than EHB at −20 °C whereas at 80 °C their diffusion coefficients are nearly identical. Again, the effect of phenyl conjugation appears to be a dominant factor in determining the difference in D between EHC and EHB at lower temperatures.

Similarly, as in our earlier study[4] of EHB, we analyzed the diffusion data in terms of the rough hard sphere (RHS) model[6] in order to gain information about the coupling of rotational and translational motions for the molecule studied. We are aware of the fact that such analysis is only approximate for the irregularly shaped flexible molecule of EHC.

The RHS theory[6] allows calculation of a theoretical diffusion coefficient of a smooth hard sphere (D_{SHS}) liquid of known molecular diameter and density according to

$$D_{SHS} = (3/8)(kT/m\pi)^{1/2}\sigma[3.7043 - 6.3355\rho\sigma^3 + 2.6718(\rho\sigma^3)^2] \quad (5)$$

where σ is the hard-sphere diameter, ρ is the number density, and the other symbols have their usual meaning. The experimental diffusion coefficient D_{exptl} is considered to be approximately equal to the rough hard sphere diffusion coefficient (D_{RHS}), which in turn is proportional to D_{SHS} by a factor A; i.e.

$$D_{exptl} \cong D_{RHS} = AD_{SHS} \quad (6)$$

The factor A can range from 0 to 1 and is considered a measure of the rotational–translational coupling of the system; the smaller the value of A, the stronger the coupling is considered to be (i.e., the fluid is diffusing less rapidly than would a smooth hard sphere).

Values of hard-sphere diameters were determined by the fluidity analysis method of Hilderbrand et al.[27] Fluidity ($\phi = 1/\eta$) was plotted against molar volume (V) for each isotherm. The linear low-density region of each plot was then extrapolated to the x axis. The hard-sphere diameter was then determined from definitions

(25) Lowitz, D. A.; Spencer, J. W.; Webb, W.; Schiessler, R. W. *J. Chem. Phys.* **1959**, *30*, 73.
(26) Cutler, W. G.; McMickle, R. H.; Webb, W.; Schiessler, R. W. *J. Chem. Phys.* **1958**, *29*, 727.
(27) Hilderbrand, J. H.; Lamoreaux, R. H. *Proc. Natl. Acad. Sci. U.S.A.* **1972**, *69*, 3428.

TABLE IV: Calculated Smooth Hard Sphere Diffusion Coefficients, Packing Fractions, and Values of A

P, bar	T, °C	packing fraction	$10^5 D_{SHS}^{EHC}$, cm^2 s^{-1}	A	packing fraction	$10^5 D_{SHS}^{EHB}$, cm^2 s^{-1}	A
1	40	0.501	1.45	0.21	0.506	1.26	0.24
1	80	0.485	2.23	0.32	0.468	3.03	0.21
500	80	0.502	1.51	0.28	0.487	2.11	0.20
1000	80				0.502	1.49	0.18

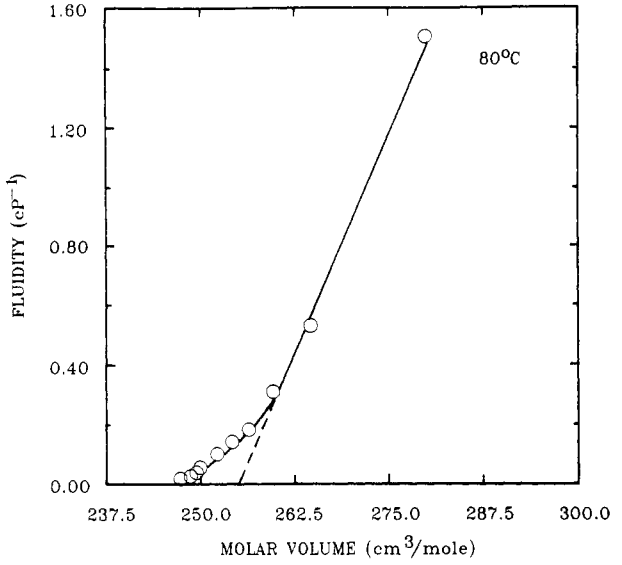

Figure 5. Volume dependence of EHC fluidity at 80 °C.

provided by Dymond's[28] $I = 1.384V_0$, $V_0 = N\sigma^3/2$, I being the x intercept, V_0 the volume of the liquid during close packing, and N Avogadro's constant. Figure 5 shows plots of fluidity versus molar volume for two of the three temperatures studied. Intercepts could only be ascertained at 80 and 40 °C due to the high curvature throughout the −20 °C plot. The analysis gave hard-sphere diameters of 7.47 Å for 80 °C and 7.51 Å for 40 °C. Comparing this with the EHB diameters[4] of 7.23 Å for 80 °C and 7.34 Å for 40 °C, it seems that there is a stronger temperature dependence on molecular diameter in EHB.

Smooth hard sphere diffusion coefficients, packing fractions, and corresponding values of A within the applicability region of (5) are shown in Table IV. Values calculated from the EHB study[4] are also given.

Table IV shows that EHC, like EHB, possesses a high degree of rotational–translational coupling. The data suggest that the degree of rotational–translational coupling is higher in EHB than in EHC. Because the low values of A in both systems undoubtedly originate from the nonspherical shape of the molecules, the differences in the A values between EHC and EHB may reflect differences in the shapes of the two molecules. As we already mentioned, EHC is more flexible than EHB due to the aromatic ring in the latter case. The EHB molecule should therefore be more rigid than EHC particularly at low temperatures, as the aromatic ring is planar, and its presence would probably add a double-bond character to the bond between the ring and the carbonyl carbon. It is also apparent that the A values for EHC at 80 °C are density dependent in agreement with the trend found at 80 °C for EHB. Since it is unlikely that σ is appreciably density dependent, as discussed before,[4] one concludes that the magnitude of rotational–translational coupling increases at higher densities.

The next part of our analysis employs the Stokes–Einstein equation

$$D = kT/(C\pi a\eta) \tag{7}$$

where a is the hydrodynamic radius, η the viscosity, and C the Stokes–Einstein constant. The value of C theoretically ranges from 4, the slipping boundary limit, to 6, the sticking boundary limit. The slip limit condition is approached when the solute and solvent are of similar size (self-diffusion) and the stick limit can be thought of as the condition where a large particle diffuses a continuum.[29] The equation has been found to be applicable in describing diffusion in simple fluids like cyclohexane,[30] methylcyclohexane,[31] and benzene[32] as well as in the more complex EHB system.[4]

TABLE V: Stokes–Einstein Constants for EHC

P, bar	−20 °C	40 °C	80 °C
1	3.4	2.9	3.9
500	2.8	2.9	4.3
1000	2.0	2.5	4.2
1500		3.1	3.6
2000		3.0	4.3
2500	4.2	3.1	4.4
3000	5.3	3.7	3.6
3500	5.0		3.2
4000	5.2		3.4
4500	5.8		4.1

As in the EHB study,[4] we have used the experimental EHC diffusion coefficients and viscosities to calculate the Stokes–Einstein constants. An average value of $a = 3.75$ Å for the EHC radius was used for all temperatures. The uncertainties in C are estimated at ±30% for the $T_{1\rho}$-derived data and ±14% for the spin-echo-derived data. The constants are shown in Table V.

It can be seen from Table V that, at 40 and 80 °C, the Stokes–Einstein equation provides a generally good description of diffusion over the corresponding viscosity range. All values of C at 80 °C approach the slipping boundary limit of 4, as would be expected in the case of self-diffusion. At 40 °C, the values of C typically fall short of the slip limit to about $C \cong 3$. It is interesting to consider, though, the microfriction correction to the Stokes–Einstein equation as proposed by Gierer and Wirtz:[33]

$$D = \frac{kT}{6\pi a\eta f} \tag{8}$$

$$f = \left(1.5\frac{a_2}{a_1} + \frac{1}{1 + \frac{a_2}{a_1}}\right)^{-1} \tag{9}$$

where a_1 and a_2 are the solute and solvent radii, respectively. Since $a_1 = a_2$ in the case of self-diffusion, $f = 1/2$ and C would be equivalent to 3. Spernol and Wirtz[34] empirically found f to be approximately 0.56 for solutions where $a_1/a_2 \cong 1.0$.[31] This would make $C = 3.36$.

The −20 °C values of C for EHC seem to start out below the slip limit and approach the stick condition. The higher density C values do originate from $T_{1\rho}$-derived data and are subject to greater error, and therefore, we do not feel justified in discussing this trend.

^{13}C Relaxation Measurements

Figure 6, which gives the natural-abundance ^{13}C NMR spectra of liquid EHC and EHB obtained at 80 °C and 5000 bar pressure, illustrates the excellent resolution obtainable even under high-pressure conditions without sample spinning. This high resolution permits T_1 measurements for each individual carbon in EHC and EHB and makes it possible to probe directly the overall and

(28) Dymond, J. H. *J. Chem. Phys.* **1974**, *60*, 969.

(29) Tyrell, H. J. V.; Harris, K. R. *Diffusion in Liquids*; Butterworths: London, 1984; p 259.
(30) Jonas, J.; Hasha, D.; Huang, S. G. *J. Phys. Chem.* **1980**, *84*, 109.
(31) Jonas, J.; Hasha, D.; Huang, S. G. *J. Chem. Phys.* **1979**, *71*, 3996.
(32) Parkhurst, Jr. H. J.; Jonas, J. *J. Chem. Phys.* **1975**, *63*, 2698.
(33) Gierer, A.; Wirtz, K. *Z. Naturforsch.* **1953**, *A8*, 532.
(34) Spernol, A.; Wirtz, K. *Z. Naturforsch.* **1953**, *A8*, 522.

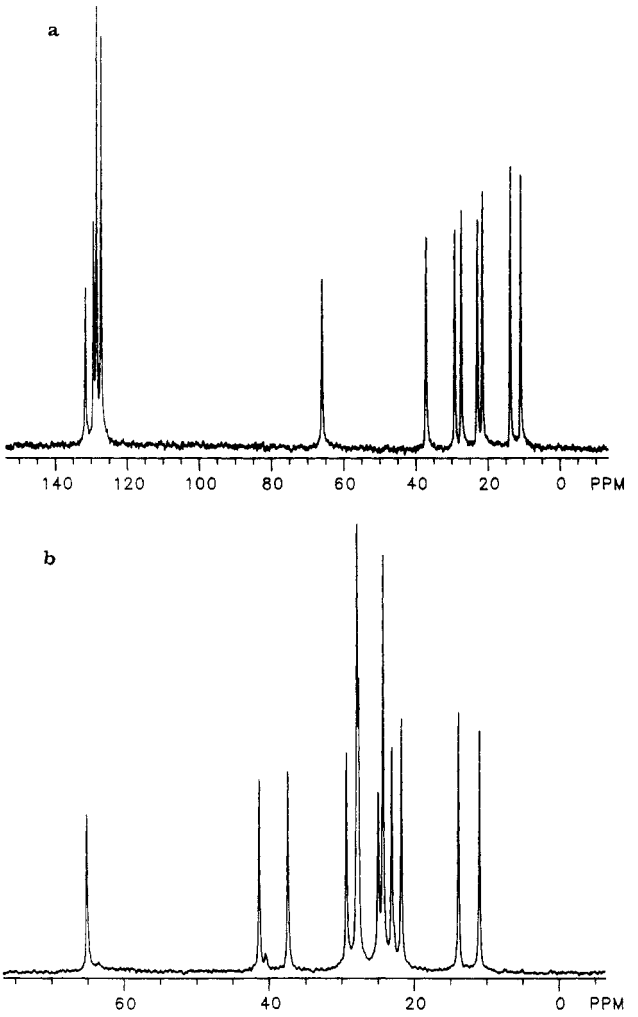

Figure 6. High-resolution natural-abundance ^{13}C NMR spectra of EHB (a) and EHC (b) at 80 °C and 5000 bar (carbonyl resonance not included).

TABLE VI: Carbon-13 Chemical Shift Assignments

carbon no.[a]	chemical shift, ppm, rel to TMS	
	EHB	EHC
2	130.8	43.1
3, 7	128.1	29.2
4, 6	129.6	25.6
5	132.4	26.1
8	66.6	65.8
9	39.0	39.3
10	30.6	34.2
11	29.0	29.2
12	23.0	23.1
13	13.9	13.8
14	24.0	24.1
15	10.9	10.9

[a] See Figure 1 for numbering of the carbons.

internal motions in these complex liquids. The fact that our experiments cover both the motionally narrowed regime and the slow-motion regime as viscosity changes extend over 5 orders of magnitude will enable us to test rigorously the various theoretical models proposed to describe the dynamics of complex molecules of asymmetric shape and high flexibility. However, in this report we discuss only the general trends in the T_1 values for individual carbons concentrating on the high-temperature limit of 80 °C of our measurements in the motionally narrowed regime (NOE ≅ 2.98). The pressure dependence of the $1/NT_1$ values for selected carbons 5, 9, and 13 in EHC and EHB at 80 °C is plotted in Figure 7. Inspection of Figure 7 shows that for the para ring

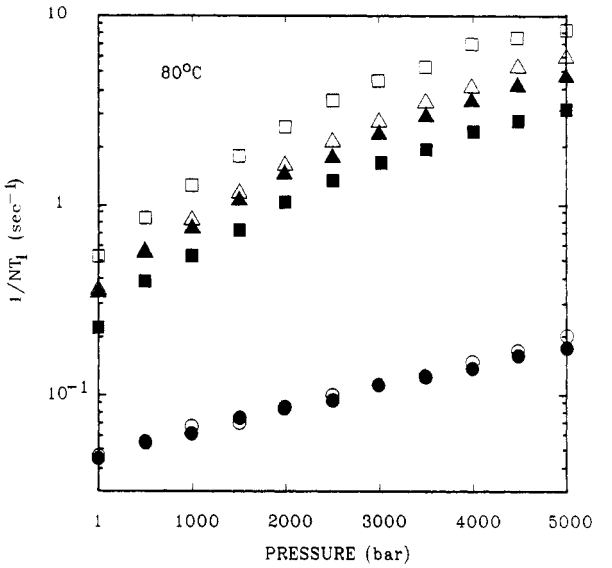

Figure 7. Pressure dependence of $1/NT_1$ for selected carbon atoms of EHB (open symbols) and EHC (full symbols) at 80 °C. EHB: □, C-5; △, C-9; ○, C-13. EHC: ■, C-5; ▲, C-9; ●, C-13. (See Figure 1 for numbering of carbon atoms.)

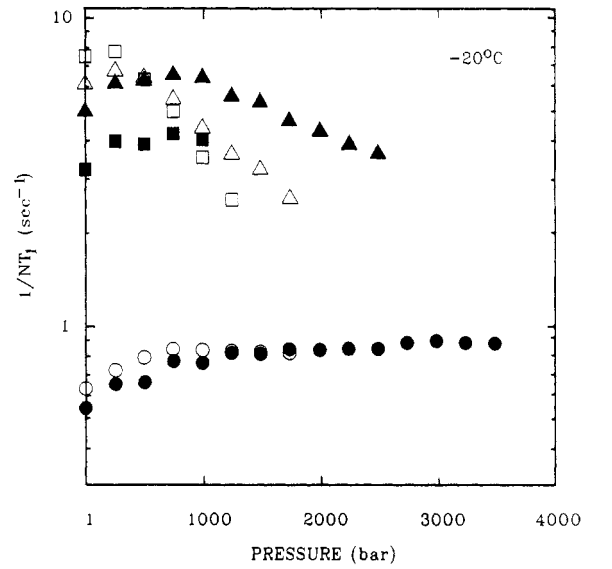

Figure 8. Pressure dependence of $1/NT_1$ for selected carbon atoms of EHB (open symbols) and EHC (full symbols) at −20 °C. EHB: □, C-5; △, C-9; ○, C-13. EHC: ■, C-5; ▲, C-9; ●, C-13. (See Figure 1 for numbering of carbon atoms.)

carbon (5) and the methine chain carbon (9) the $1/NT_1$ values for EHB are higher than the corresponding values for EHC, reflecting the higher mobility of the cyclohexyl ring. It is interesting to find that $1/NT_1$ values for EHB are larger than those for EHC even at 80 °C in spite of the fact that the viscosities of EHB and EMB are nearly identical at this temperature. It is not surprising that the side-chain methyl group has nearly identical $1/NT_1$ values both for EHC and EHB due to the high C_3 symmetry of the end CH_3 group and high flexibility of the chain. Figure 8 was included to show that at −20 °C the motions of both EHB and EHC falls into the slow-motion regime.

As we mentioned, the NOE's values determined for each individual carbon at 80 °C indicate that at least for this temperature the extreme narrowing condition is valid $(\omega_c + \omega_H)^2\tau \ll 1$. As a first approximation, we can calculate[10,11] the effective rotational correlation time τ_{eff} for the vector connecting the directly bonded C and H atoms, according to

$$\tau_{eff} = r_{CH}^6/CT_1N \qquad (10)$$

where r_{CH} is the internuclear distance (1.09 Å for aliphatic C–H

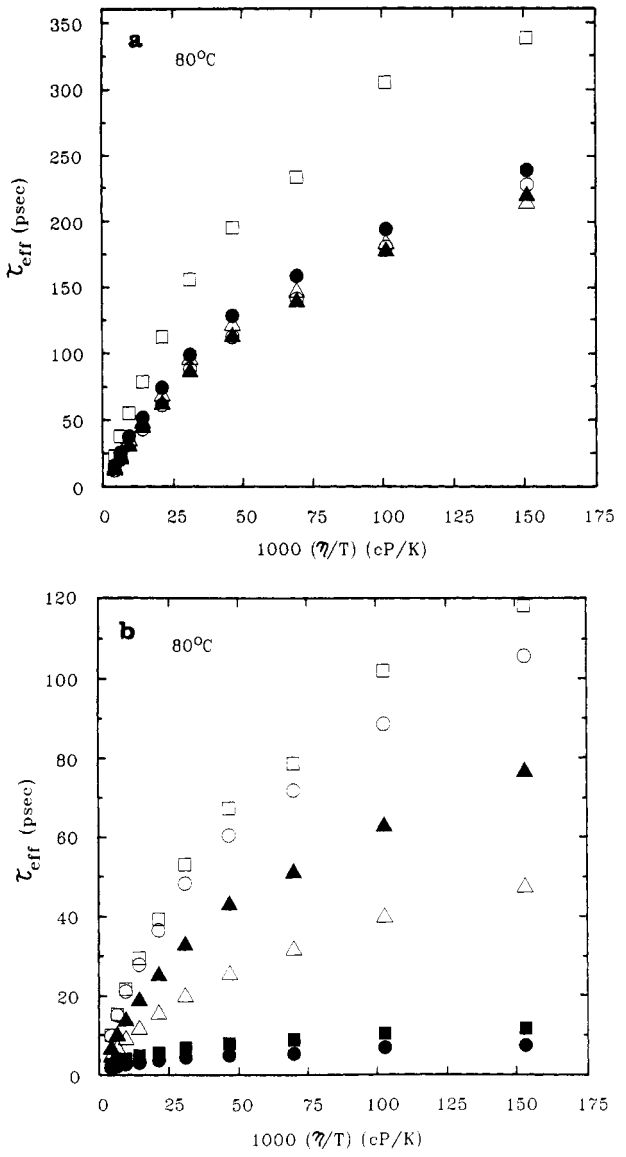

Figure 9. Effective rotational correlation time, τ_{eff}, as a function of η/T for EHB at 80 °C. (a) □, C-5; ▲, C-4,6; ○, C-3,7; △, C-8; ●, C-9. (b) □, C-10; ▲, C-11; ○, C-14; △, C-12; ●, C-13; ■, C-15. (For numbering of carbon atoms see Figure 1.)

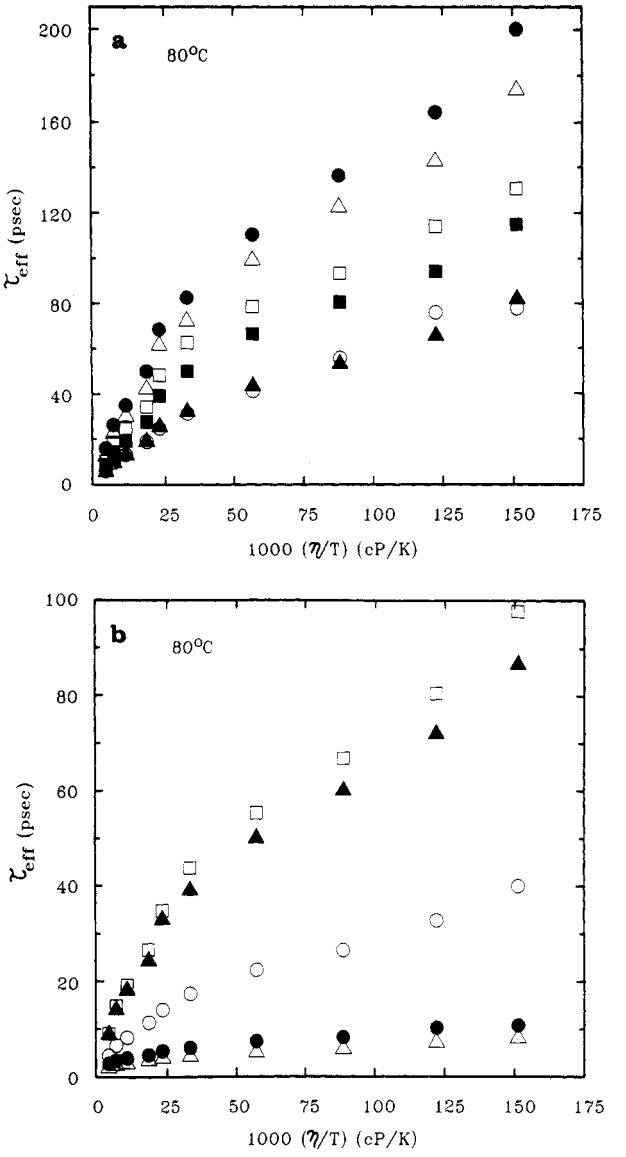

Figure 10. Effective rotational correlation time, τ_{eff}, as a function of η/T for EHC at 80 °C. (a) □, C-5; ▲, C-4,6; ○, C-3,7,11; △, C-8; ●, C-9; ■, C-2. (b) □, C-10; ▲, C-14; ○, C-12; △, C-13; ●, C-15. (For numbering of carbon atoms see Figure 1.)

groups and 1.08 Å for aromatic C–H groups), T_1 is the spin–lattice relaxation time, N is the number of attached protons, and C is a constant equal to 3.56×10^{10} Å^6 s^{-2}. In order to check the applicability of the modified Debye equation (1), we plot τ_{eff} as a function of η/T at 80 °C for the individual carbon atoms in EHB and EHC in Figures 9 and 10. One should point out that the single correlation time τ_{eff} as given in (10) approximates in fact a weighted average of correlation times which characterize the motion of the C–H vector.

The functional dependence of the effective rotational correlation time τ_{eff} upon η/T resembles the typical τ_θ vs η/T dependence found for molecules[8] that have an axis of symmetry about which the reorientation is relatively unhindered. However, this characteristic dependence was observed for rigid molecules whereas EHB and EHC are asymmetric highly flexible molecules, and therefore, one has to take this fact into consideration when discussing the decoupling of rotational and translational motions at higher viscosities.

With increasing η/T values, the parameter κ (see (1)), which characterizes the coupling between the rotational and translational motions for individual carbons, decreases. This observation is seemingly in contrast with the results of the RHS analysis of the diffusion data and viscosity data which indicated that the rotational–translational coupling increases with increasing pressure. However, one must realize that the RHS approximative analysis yields information about the rotational–translational coupling between overall rotation of the complex molecule, whereas the τ_{eff} values for individual C–H vectors describe both overall and multiple internal rotations. Therefore, it is not surprising that one finds κ for individual carbons decreasing with increasing η/T as the individual side-chain carbons can undergo complex internal rotations resulting in decreased coupling to translational motions of the complex molecule. The behavior of τ_{eff} for the methyl carbons represents an extreme as over a wide range of viscosities the very low value of κ is essentially independent of η/T.

As already mentioned in connection with the $1/NT_1$ dependence upon pressure at 80 °C depicted for EHB and EHC in Figure 7, the relaxation rate $1/NT_1$ is higher for specific carbons in EHB than in EHC in spite of the fact that viscosities are essentially identical for these two complex liquids at 80 °C. Similarly, for high values of η/T, Figure 9 shows that τ_{eff} for carbons 2–8 in EHB is in the range of 200–340 ps, whereas the observed τ_{eff} for the same carbons ranges from 60 to 200 ps.

As an approximation to evaluating the relative mobility of the individual carbon atoms, we may consider the slopes of the τ_{eff} vs η/T plots, which according to (1) give the parameter κ, a measure of the rotational–translational coupling. The general behavior is as expected, because the further the carbon atom is

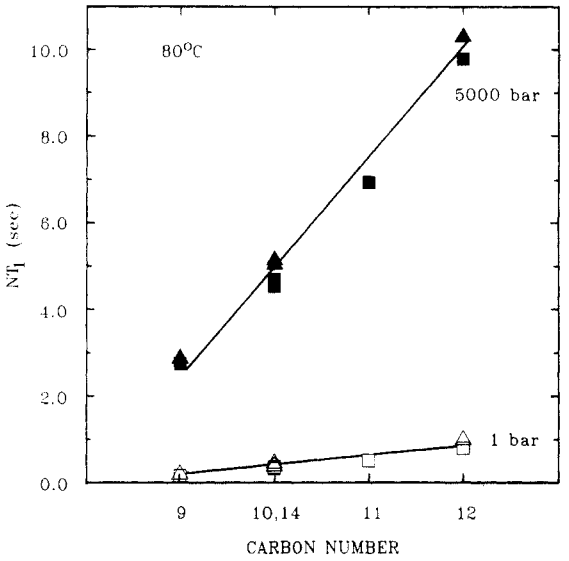

Figure 11. Dependence of NT_1 for chain carbons in EHB and EHC at 80 °C for 1 and 5000 bar: ■, EHB, 80 °C, 1 bar; □, EHB, 80 °C, 5000 bar; ▲, EHC, 80 °C, 1 bar; △, EHC, 80 °C, 5000 bar.

along the ethylhexyl chain, the lower the parameter κ. This signifies that its mobility is higher. In agreement with this approximative evaluation of relative mobilities are the values of $R = \tau_{min}/\tau_D$, where τ_{min} is the correlation time, calculated[35] from the T_1 minimum at lower temperature, where $\omega\tau_{min} = 0.6158$ and τ_D is the correlation time calculated from the Debye equation. For example, at −20 °C for EHB the R values for individual carbons exhibit the following progression $R(5) \cong > R(3,7) \cong R(4,6) > R(10,14) > R(11,12,13,15)$. The detailed analysis of κ and R values will be given in detail elsewhere.[36]

The data presented in Figure 9 and 10 also suggest that the ring and the whole molecule are undergoing anisotropic reorientation, and the aliphatic chain is undergoing multiple internal rotations about each C–C bond. Figure 11 gives a good graphical illustration of the mobility gradient along the chain with the chain mobility increasing as one moves away from the methine carbon (carbon 9, Figure 1). A plot of NT_1 vs carbon number, starting with the methine carbon 9 shows a linear dependence. According to the model for multiple internal rotations,[14] this observation is indicative of equal rotational diffusion constants for all bonds in the chain except for the terminal methyl group. An increase in slope indicates that the rotational diffusion constant increases for all carbons, and this behavior persists even at the high pressure of 5000 bar.

Preliminary theoretical analysis of the T_1 and NOE data shows that both simple models involving overall and internal rotation and models involving anisotropic reorientations with multiple internal rotations do not reproduce the experimental data. It appears that one has to use a Cole–Davidson distribution[37] of correlation times. This approach has successfully been used in our laboratory to interpret the temperature and pressure dependence of deuterium relaxation times in selectively deuterated glycerols.[38] Availability of T_1 and NOE values for fluidity changes of 5 orders of magnitude offers a unique opportunity not only to test rigorously various theoretical models for dynamics of complex liquids but, for the first time, these experiments will allow one to characterize the density and temperature effects on the molecular dynamics in complex liquids. Theoretical analysis of the experimental T_1 and NOE data is in progess[36] in our laboratory.

Acknowledgment. This research was partially supported by the Air Force Office for Scientific Research under Grant AFOSR 89-0099 and the National Science Foundation under Grant NSF CHE 85-09870 and Grant NSF DMR 86-12860 and Shell Research (U.K.).

(35) Jonas, J.; Arndt, E. R. *J. Magn. Reson.* **1978**, *32*, 297.
(36) Adamy, S.; Grandinetti, P. J.; Masuda, Y.; Campbell, D. Manuscript in preparation.
(37) Davidson, D. W.; Cole, R. M. *J. Chem. Phys.* **1951**, *19*, 1484.
(38) Wolfe, M.; Jonas, J. *J. Chem. Phys.* **1979**, *71*, 3252.

Experimental Studies on the Rheology of Hard-Sphere Suspensions near the Glass Transition

Louise Marshall and Charles F. Zukoski IV*

Department of Chemical Engineering, University of Illinois, Urbana, Illinois 61801 *(Received: July 17, 1989)*

We have investigated the rheological behavior of sterically stabilized colloidal silica particles of three different sizes at volume fractions above 0.5. Despite a small surface charge, which elevated the intrinsic viscosity from the Einstein value of 2.5, the particles were found to behave essentially as hard spheres in the concentrated suspensions and to have properties highly reminiscent of molecular glasses. The zero shear rate viscosity, characteristic of disordered suspensions and present at all volume fractions, diverges as $\phi \rightarrow 0.6$ and is well-described by the Doolittle equation for glassy flow. For suspensions with a relative zero shear rate viscosity greater than 5×10^2, shear thickening was observed. Characteristic time scales for particle rearrangement determined from critical shear rates for shear thinning and shear thickening were found to follow trends predicted for molecular glasses. A transition from a liquidlike linear relaxation response to glassy stretched exponential behavior was observed as volume fraction was increased. The onset of the glassy relaxation response, indicative of nondecaying correlations, occurred near a volume fraction of 0.52.

I. Introduction

Computer simulation and analytical studies of hard-sphere liquids have provided many insights into the origins and manifestations of the glass transition.[1-3] These studies suggest that hard-sphere liquids fall out of equilibrium with the liquid state into a metastable vitreous phase (i.e., undergo a phase transition) at volume fractions between 0.50 and 0.64. The broad range of transition volume fractions arises from the different methods of

(1) Woodcock, L. V. *Ann. N.Y. Acad. Sci.* **1981**, *37*, 274.
(2) Jäckle, J. *Rep. Prog. Phys.* **1986**, *49*, 171.
(3) Angell, C. A.; Clarke, J. H. R.; Woodcock, L. V. *Adv. Chem. Phys.* **1981**, *48*, 397.

0022-3654/90/2094-1164$02.50/0